

RESEARCH LETTER

10.1002/2013GL058979

Key Points:

- Wet-surface temperature stays near-constant with distance to moisture jump
- Aridity changes cannot alter the temperature of a freely evaporating surface
- Wet-surface temperature can be estimated from any stage of drying

Correspondence to:

J. Szilagyi,
jszilagy1@unl.edu

Citation:

Szilagy, J., and A. Schepers (2014), Coupled heat and vapor transport: The thermostat effect of a freely evaporating land surface, *Geophys. Res. Lett.*, *41*, doi:10.1002/2013GL058979.

Received 12 DEC 2013

Accepted 8 JAN 2014

Accepted article online 13 JAN 2014

Coupled heat and vapor transport: The thermostat effect of a freely evaporating land surface

Jozsef Szilagyi^{1,2} and Aaron Schepers³

¹Department of Hydraulic and Water Resources Engineering, Budapest University of Technology and Economics, Budapest, Hungary, ²Conservation and Survey Division, School of Natural Resources, University of Nebraska, Lincoln, Nebraska, USA, ³Cornerstone Mapping, Inc., Lincoln, Nebraska, USA

Abstract Analytical solutions of the 2-D heat and vapor transport equations for a surface moisture jump are often based on a constant streamwise temperature (T_{ws}) assumption over the wet vegetated surface. By analyzing 90 thermal infrared images taken over center-pivot irrigated areas in Nebraska, it has been demonstrated for the first time that such an assumption is realistic. Average temperature difference between the perimeter and core of the irrigated full or half circles stayed between -0.11 and 0.09°C (standard deviation of 0.25 – 0.41°C). It was further demonstrated that wet-bulb temperatures (a proxy of T_{ws}) remain near constant during drying of the environment when net radiation and wind conditions stay largely unchanged, enabling estimation of T_{ws} at any stage of drying, thus improving evaporation estimates of the Priestley-Taylor equation in arid and semiarid environments.

1. Introduction

Analytical solutions of the classical steady state 2-D vapor and/or heat transport equations written for a sudden, constant jump in surface moisture and/or temperature, T_s , are still used in tackling practical problems across a variety of disciplines [Kunsch, 1998; Szilagyi and Jozsa, 2009a, 2009b; Bhat et al., 2011]. The equations in short-hand notation can be written as

$$u(z) \frac{\partial[q(x, z), \Theta(x, z)]}{\partial x} = \frac{\partial}{\partial z} \left(K(z) \frac{\partial[q(x, z), \Theta(x, z)]}{\partial z} \right) \quad (1)$$

where u is mean horizontal wind velocity across the surface-property jump taken over a suitable time interval, q is mean specific humidity, Θ is mean potential temperature, K is eddy diffusivity, x and z are horizontal and vertical coordinate references, $x = 0$ at the surface-property jump, and $x > 0$ at points downwind over the wet surface. See Brutsaert [1982] for an exhaustive description and historical background of the theory.

When the vapor transport or the coupled equations are written for a freely evaporating vegetated land area (assuming negligible ground heat conduction) within a drier environment, a spatially constant temperature, T_{ws} , as a concentration-type boundary condition, is often prescribed for the wet surface [Sutton, 1934; Philip, 1959; Rider and Philip, 1960; Rider et al., 1963]. Rider and Philip [1960] argue that “the most important factor operating in advective evaporative effects is the change in the partition of available energy” (R_n) between the sensible (H) and latent heat (LE) terms, while any simultaneous change in R_n remaining secondary. If it is true that advective effects can only partition R_n at a homogeneous wet surface, then it follows that R_n and T_{ws} must be constant along it [Rider et al., 1963]. One can argue that this picture is simplistic because several important environmental aspects are not accounted for. McNaughton [1976] gives a summary of the factors not represented in the classical theory of advection: changes in roughness height, eddy diffusivity, and mean wind speed across the surface-property jump being chief among them. So can these combined factors become significant enough to render the constant T_{ws} assumption a convenient but somewhat artificial condition for obtaining a tractable analytical solution and thus make the practical value of any work that build upon it less convincing? Or is it possible that a constant T_{ws} is real and observable in nature? While Brutsaert [1982, chapter 7.2a] declares a constant T_{ws} assumption (meaning the lack of a spatial trend over the surface while allowing for random T_{ws} variations) “probably quite satisfactory” over “an irrigated field in an arid environment,” such as studied by Rider et al. [1963], there has been no concrete evidence that such a condition exists, which motivates the present study. A spatially constant T_{ws} implies the possible invariance of T_{ws} to the drying out of the environment (first hypothesized by Szilagyi and Jozsa [2008] for constant R_n and wind),

Table 1. Instantaneous T_a , T_d , Wind Speed, and Direction Values From Automated Surface Observation Stations at Broken Bow and Grand Island (Figure 1) at the Time of Measurement Closest to the Starting and Ending Times of T_s Data Acquisition^a

Date 2011	No. of T_s Observed	Starting/Ending Time (Local)	Ranges												No. of Irrigated Areas
			Broken Bow						Grand Island						
			T_a (°C)	T_d (°C)	Wind Speed (ms ⁻¹)	Direction (Degree From North)	T_a (°C)	T_d (°C)	Wind Speed (ms ⁻¹)	Direction (Degree From North)	Mean T_s	Std (°C)			
8 July	1	12:44	25.6	18.9	8.8	190	28.9	18.9	5.7	190	24.25	0	1		
19 July	3	12:26–15:07	32.2–33.3	22.2–22.2	5.1–6.2	200–180	33.9–35.6	21.1–21.1	7.2–6.7	190–180	26.16	1.11	6		
5 September	1	15:40	22.8	7.8	6.7	150	21.7	7.2	4.1	140	20.32	0	1		
6 September	3	10:24–11:11	18.3–18.3	6.7–6.7	6.2–6.2	190–190	18.3–18.3	8.9–8.9	6.2–6.2	180–180	16.18	0.41	3		
8 September	27	10:05–12:25	17.1–22.2	11.0–8.9	0–2.6	N/A–150	17.8–22.8	12.2–10.0	1.5–3.6	340–10	16.84	1.36	28		
12 September	41	10:30–12:28	25.0–31.7	9.4–9.4	3.1–3.6	Varies–280	26.1–29.4	10.6–12.2	7.2–5.1	220–200	22.01	1.44	51		

^aStd is the standard deviation of the T_s values.

enabling the estimation of T_{ws} at any stage of drying. Such T_{ws} values have been demonstrated to improve evapotranspiration estimates [Szilagyi et al., 2009; Huntington et al., 2011; McMahon et al., 2013].

2. T_s Measurements Over Freely Evaporating Areas Within a Drier Environment

In the growing season center-pivot irrigated crop circles of different size are in stark contrast with their environment in arid and semiarid climates in terms of their soil moisture and temperature. The center pivot can deliver the water evenly over the irrigated area resulting in fairly homogeneous crop fields with a typically well defined edge, which makes them an ideal tool for testing the constant T_{ws} hypothesis.

T_s measurements in semiarid central Nebraska took place between 10 A.M. and 4 P.M. local time on rainless days of July and September 2011 (Table 1) from an airplane of Cornerstone Mapping Inc. (www.cornerstonemapping.com) flying at an altitude of 4000 m in July and 3600 m in September, using a Jenoptik thermal infrared camera with sensitivity of 0.07°C, yielding a spatial resolution of 2 m in July and 1.8 m in September by the 640 × 480 pixels of each picture taken. The brightness temperature values were corrected for target emissivity. Note that further accounting for atmospheric attenuation is not necessary because only those temperature values are compared to each other in the ensuing analysis that were obtained at the same time, i.e., belong to the same irrigated field. From the available images only the ones that contained the bulk of at least one center-pivot area were selected with special emphasis to exclude fields situated within an extensive irrigated region in order to allow for significant energy advection (Figure 1). Figure 2 displays four of the 90 center-pivot areas that were analyzed.

T_{ws} values of the images were averaged for 10 equal areas, encompassed by concentric circles between ~0.9 and 0.05 times the radius (R) of the irrigated fields with an observed range of 360 to 420 m (Figure 2). The outermost circle was necessary to be defined less than R because of frequent intrusions of drier land areas into the perimeter of the irrigated region, typically in the form of roads, agricultural buildings, or homes, as seen in Figure 2. T_{ws} values were also averaged separately on the half of the circles that were facing the prevailing wind at the time of the measurements in order to see if there was any difference in outcomes.

In the study of Davenport and Hudson [1967] conducted during the winter months in the semiarid Gezira region of the Sudan, early afternoon air temperature, T_a , measured at 2 m above ground, fell from about 29°C to 24°C on a typical day over a 300 m irrigated cotton field. The corresponding decrease in evaporation rate (E) was found to be from 13 to 7.5 mm d⁻¹ (the last ~25% of the drop taking place between 40 and 300 m from the edge of the field). In the study by Lang et al. [1974] in a semiarid region of Australia, E dropped by 50% along a distance of 500 m over an irrigated rice field, with mean daily leading-edge T_a within the range of 15.1–26.6°C and corresponding E

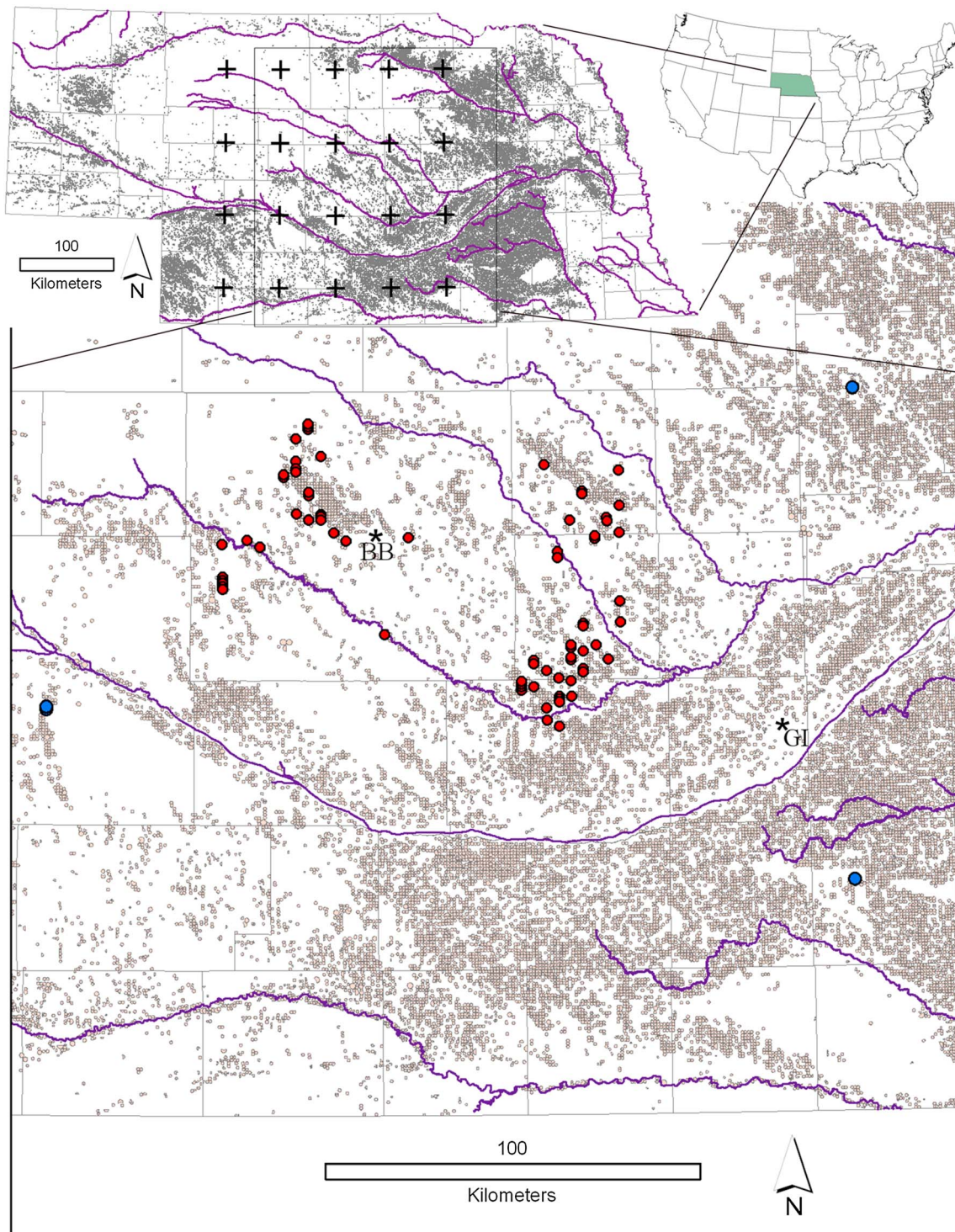


Figure 1. Distribution of center-pivot irrigation systems in central Nebraska with the locations of 76 thermal infrared image acquisitions yielding 90 center-pivot irrigated areas for analysis. Small, red circles: September 2011; blue circles: July 2011. Automated surface observation weather stations are at Broken Bow (BB) and Grand Island (GI). The large crosses are the centers of the ERA-Interim reanalysis grid cells with spatial resolution of 0.7° chosen for testing the time-invariant T_{ws} hypothesis.

between 5.43 and 9.92 mm d^{-1} (the last $\sim 30\%$ of the drop occurring between $40\text{--}400 \text{ m}$ from the edge of the field). Clearly, at the leading edge of the wet-surface, E is boosted by a reversed H flux resulting from the hot air overrunning the colder wet surface, as evidenced in Table 1, the T_{ws} values always staying below T_a , even though the latter is measured at a distance above the hot and relatively dry surface.

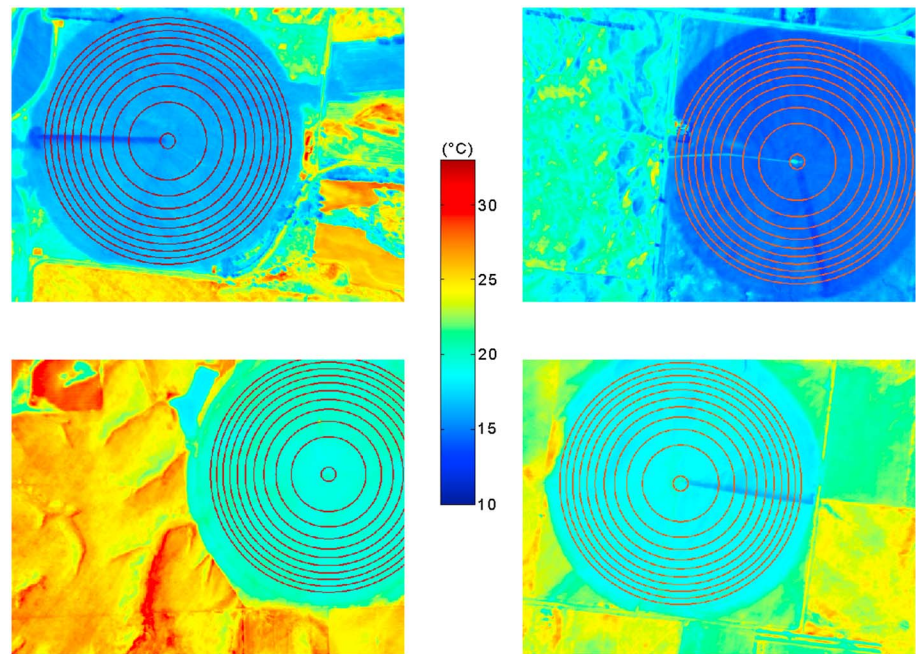


Figure 2. Selected thermal infrared images for September 2011. Spatial resolution is 1.8 m. The concentric circles encompass equal areas with the exception of the innermost one, necessary to block out high values around the center-pivot engine house. Temperature values were spatially averaged taking into account (a) all pixel values within each annulus and (b) pixel values within each semiannulus facing the prevailing wind at the time of image acquisition.

These studies are in support of the present “experimental setup” in the sense of aridity of climate, T_a range, air stability, and especially the size of the irrigated fields over which, if T_{ws} does change with distance to the edge, it ought to be detectable by the employed high-sensitivity thermal infrared imaging. Table 1 summarizes the environmental conditions on the days of image acquisition.

Figure 3a displays the resulting averages by month and spatial averaging employed, as normalized values to detect any trend in the values. The September measurements ($n = 83$) display a slight but statistically significant decreasing trend toward the center, most probably due to soil moisture limitations, because the irrigation season typically ends by September in Nebraska. According to theory [Sutton, 1934; Philip, 1959], the perimeter evaporates at a faster rate than the core while soil moisture is not limiting, leading to faster moisture depletion, thus, in time cutting back on E , reflected by the slightly elevated T_{ws} values. The fewer July measurements ($n = 7$) do not express such a decreasing trend. Figure 3b displays the T_{ws} differences between the outermost and innermost annuli, with the corresponding standard deviations for September and July. The sample mean of the differences remain between -0.11 and 0.09°C , which is comparable to the sensitivity (i.e., 0.07°C) of the measurements. Therefore, it can be concluded that T_{ws} of the irrigated fields do not change with distance from the edge, supporting the application of a constant T_{ws} in the derivation of the aforementioned classical analytical solutions.

3. Consequences of a Spatially Constant T_{ws} of Freely Evaporating Surfaces

The near constancy of the observed T_{ws} values downwind of a sudden constant jump in moisture not only corroborates the constant concentration-type boundary condition assumption of the classical advection solutions but it also implies the following. If advection can only partition R_n at the wet surface into H and LE but cannot change T_{ws} , then it can be expected that changes in aridity (meaning simultaneous but opposite changes in T_a and humidity) alone would not influence T_{ws} as long as R_n and wind characteristics remain unchanged during dry out of the environment. Note that advection of the drier air creates its aridity gradient in space downwind of the moisture jump; thus, one sees the temperature response of the wet surface (or rather the lack of it) to changes in aridity. This tendency of the wet surface to maintain its T_{ws} both in space and time while the environment becomes hotter and drier (provided R_n and wind properties remain largely

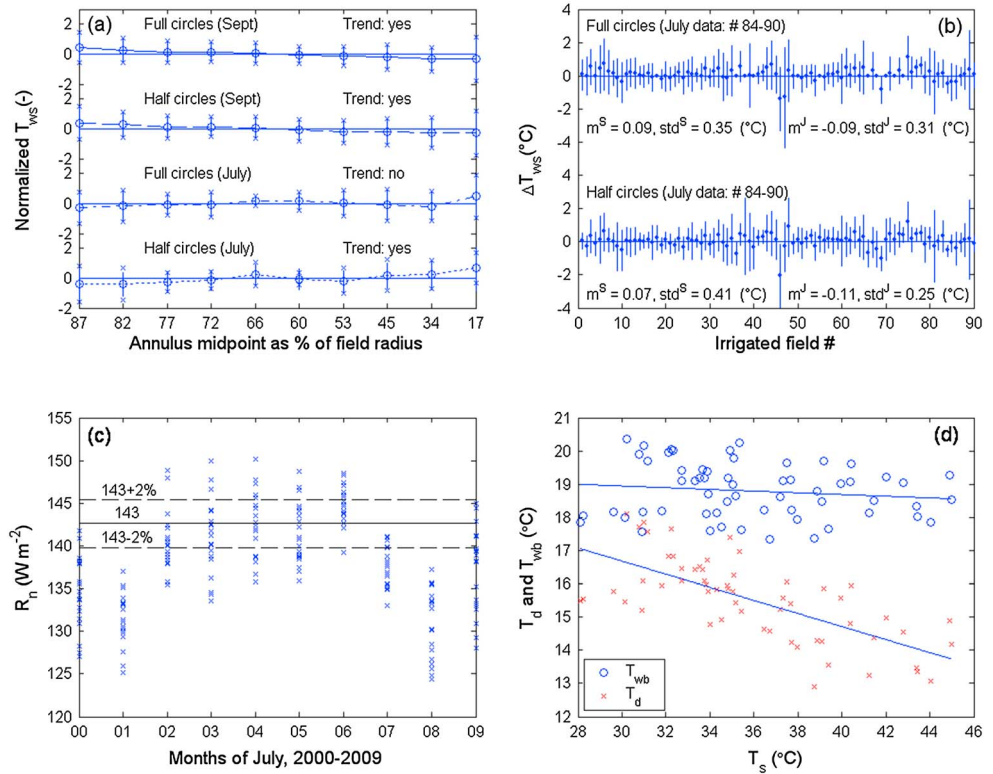


Figure 3. (a) Normalized values of spatially averaged T_{ws} taken over full or windward semiannuli of the center-pivot irrigated fields. The trend results come from the Mann-Kendall test at a 5% significance level. (b) Differences (ΔT_{ws}) in spatially averaged T_{ws} values between the outermost and innermost full or windward semiannuli. The length of each whisker designates the corresponding standard deviation for the given location. The m and std values (degree Celcius) are the sample means and standard deviations for July (J) and September (S). (c) Estimated R_n at the surface in July (2000–2009) for the ERA-Interim grid cells of Figure 1. (d) T_d and T_{wb} values for cells having $R_n = 143 \pm 2.86 \text{ W m}^{-2}$ plotted against MODIS-derived daytime T_s values of the cells ($n = 59$). The two first-order polynomials are $T_d = -0.2T_s + 22.59$ and $T_{wb} = -0.02T_s + 19.72$. Average T_{wb} is $18.8 \pm 0.82^\circ\text{C}$.

unchanged) maybe referred to as the “thermostat effect” coined by plant researchers observing quasi-constant wet leaf temperatures at T_d in excess of $30\text{--}35^\circ\text{C}$ [Spronken-Smith *et al.*, 2000].

But is it true that T_{ws} would stay constant in time during drying of the environment? Is it possible that R_n and wind remain largely unchanged during such a transition? In theory, T_{ws} changes in time could be tracked by Moderate Resolution Imaging Spectroradiometer (MODIS), but continuous surfaces of irrigated land are rarely large enough to fill the approximately 1 km by 1 km MODIS cell even within the most intensively irrigated regions in Nebraska where the almost continuous center-pivot areas are broken up by roads, buildings, and nonirrigated land patches. The larger shallow lakes (to fill in a MODIS cell), found in the Sand Hills region of central Nebraska, on the other hand, may express heat storage effects even on a monthly scale [Kovacs, 2011], affecting the T_{ws} values of the lake surface. So probably the best way of demonstrating the invariance of T_{ws} during drying is via the constancy of T_{wb} for months having similar R_n since T_{wb} and T_{ws} only differ by a constant fraction of R_n [Monteith, 1981] as long as wind conditions remain unchanged.

R_n for July of 2000–2009 was obtained by two methods over central Nebraska. First, by the WREVP program of Morton *et al.* [1985] with monthly inputs of 0.5° incident global radiation data at the surface [National Oceanographic and Atmospheric Administration, 2009], as well as air and dew point temperatures (T_d) from the PRISM Climate Group [2013] data set aggregated to the 0.5° grid. Second, it was obtained as the sum of the sensible and latent heat fluxes provided by the ERA-Interim 0.7° reanalysis data of the European Centre for Medium-Range Weather Forecasts. For a technical description of the reanalysis data, see European Centre for Medium-Range Weather Forecasts [2007]. Figure 1 displays the ERA-Interim grid centers employed.

July was chosen for analysis because irrigation in Nebraska is the most intense during this month, while T_d is the highest, yielding a large contrast between the drying and wet land surfaces. The monthly mean T_{wb} was

obtained from the wet-bulb equation [Brutsaert, 1982] employing monthly means of T_a and T_d (measured at 2 m above the ground) aggregated to the ERA-Interim cells as

$$T_{wb} \approx \frac{\gamma T_a + T_d \Delta e_s(T_d)}{\gamma + \Delta e_s(T_d)} \quad (2)$$

where γ is the psychrometric constant and Δe_s is the slope of the saturation vapor pressure curve at T_d .

Figure 3c displays the R_n values for the ERA-Interim grid cells as the arithmetic average of the WREVAP and ERA-Interim-derived values. Cells with a July R_n value of $143 \pm 2.86 \text{ W m}^{-2}$ were selected (altogether 59), and the corresponding T_d and estimated T_{wb} values were plotted against the MODIS-derived daytime T_s values (Figure 3d), a proxy measure of aridity. With aridity increases under a quasi-constant R_n , T_d drops from about 17°C to less than 14°C (while T_s grows from 28°C to 45°C , signaling a substantial change in aridity) as the air becomes ever drier, but the corresponding T_{wb} remains practically constant at about $18.8 \pm 0.82^\circ\text{C}$, in support of a time-invariant T_{ws} .

A time-invariant T_{wb} and so T_{ws} under a quasi-constant R_n can be “back-calculated” at any stage of drying as was done by Szilagyi and Jozsa [2008], Szilagyi et al. [2009], Huntington et al. [2011], and McMahon et al. [2013]. This is of importance because many actual E estimation methods start with the Priestley and Taylor [1972] equation (PTE) parameterized with data representing wet environments yet in practice typically applied with data taken during drying surface conditions [e.g., Huntington et al., 2011]. Szilagyi and Jozsa [2008] argue that T_a is close to T_{ws} over wet surfaces having a spatial extent of a kilometer or larger, the scale PTE is valid for; thus, its application with the back-calculated T_{ws} value in place of the dry-environment T_a (in arid climates the difference may reach 10°C) can improve evaporation estimations significantly [Szilagyi and Jozsa, 2008; Szilagyi et al., 2009; Huntington et al., 2011; McMahon et al., 2013], especially in arid or semiarid environments.

4. Summary

With the help of high-accuracy thermal infrared imagery over center-pivot irrigated areas, the existence of a long-hypothesized constant streamwise T_{ws} over freely evaporating areas within a drier land was corroborated. The inability of advection to noticeably change the temperature of the freely evaporating surface, at least under summer conditions of a pasture/agricultural landscape in a semiarid climate, not only supports the applicability of the analytical solutions employing such a constant concentration-type boundary condition in the natural environment under similar conditions but also implies that T_{ws} remains largely unchanged with aridity changes of the environment as long as R_n at the surface and wind characteristics stay quasi-constant. This has been demonstrated here for T_{wb} with the help of T_a , T_d , T_s and radiation data over a large range in aridity. The time-invariant T_{ws} can be back-calculated any time for the actual R_n and wind conditions similar to T_{wb} (however not the same way), thus improving estimates of the Priestley-Taylor equation with inputs obtained under arid/semiarid conditions.

Acknowledgments

This work has been supported by the Agricultural Research Division of the University of Nebraska-Lincoln.

The Editor thanks three anonymous reviewers for their assistance evaluating this paper.

References

- Bhat, A., A. Kumar, and K. Czajkowski (2011), Development and evaluation of a dispersion model to predict downwind concentrations of particulate emissions from land application of class B biosolids in unstable conditions, in *Indoor and Outdoor Air Pollution*, edited by J. Orosa, pp. 29–40, Intech, Rijeka, Croatia. [Available at www.intechopen.com.]
- Brutsaert, W. (1982), *Evaporation Into the Atmosphere: Theory, History and Applications*, D. Reidel, Dordrecht, Netherlands.
- Davenport, D. C., and J. P. Hudson (1967), Changes in evaporation rates along a 17-km transect in the Sudan Gezira, *Agric. Meteorol.*, *4*, 339–352.
- European Centre for Medium-Range Weather Forecasts (2007), *IFS Documentation—Cy31r1, Part IV: Physical Processes*, ECMRWF, Shinfield Park, Reading, U. K.
- Huntington, J., J. Szilagyi, S. Tyler, and G. Pohl (2011), Evaluating the complementary relationship for estimating evapotranspiration from arid shrublands, *Water Resour. Res.*, *47*, W05533, doi:10.1029/W2010WR009874.
- Kovacs, A. D. (2011), Improving lake and aerial evapotranspiration estimations in Hungary, PhD dissertation, Budapest Univ. Tech. Econ., Hungary.
- Kunsch, J. P. (1998), Two-layer integral model for calculating the evaporation rate from a liquid surface, *J. Hazard. Mater.*, *59*, 167–187.
- Lang, A. R. G., G. N. Evans, and P. Y. Ho (1974), The influence of local advection on evapotranspiration from irrigated rice from a semi-arid region, *Agric. Meteorol.*, *13*, 5–13.
- McMahon, T. A., M. C. Peel, and J. Szilagyi (2013), Comment on the application of the Szilagyi–Jozsa advection–aridity model for estimating actual terrestrial evapotranspiration in “Estimating actual, potential, reference crop and pan evaporation using standard meteorological data: A pragmatic synthesis” by McMahon et al. (2013), *Hydrol. Earth Syst. Sci.*, *17*, 4865–4867.
- McNaughton, K. G. (1976), Evaporation and advection I: Evaporation from extensive homogeneous surfaces, *Quart. J. Roy. Meteorol. Soc.*, *102*, 181–191.
- Monteith, J. L. (1981), Evaporation and surface temperature, *Quart. J. Roy. Meteorol. Soc.*, *107*, 1–27.

- Morton, F. I., F. Ricard, and F. Fogarasi (1985), Operational estimates of areal evapotranspiration and lake evaporation—Program WREVAP, National Hydrologic Research Institute Paper no. 24, NHRI, Saskatoon, Canada.
- National Oceanographic and Atmospheric Administration (NOAA) (2009), Surface radiation budget data. [Available at <http://www.atmos.umd.edu/~srb/gcip/cgi-bin/historic.cgi>.]
- Philip, R. J. (1959), The theory of local advection: I, *J. Meteorol.*, *16*, 535–547.
- Priestley, C. H. B., and R. J. Taylor (1972), On the assessment of surface heat flux and evaporation using large-scale parameters, *Mon. Weather Rev.*, *100*(2), 81–92.
- PRISM Climate Group (2013), Climate data, Oregon State University. [Available at <http://prism.oregonstate.edu>.]
- Rider, N. E., and R. J. Philip (1960), Advection and evaporation, *Assoc. Int. Hydrol. Sci.*, *53*, 421–427.
- Rider, N. E., J. R. Philip, and E. F. Bradley (1963), The horizontal transport of heat and moisture—A micrometeorological study, *Q. J. R. Meteorol. Soc.*, *89*, 507–531.
- Spronken-Smith, R. A., T. R. Oke, and W. P. Lowry (2000), Advection and the surface energy balance across an irrigated urban park, *Int. J. Climatol.*, *20*, 1033–1047.
- Sutton, O. G. (1934), Wind structure and evaporation in a turbulent atmosphere, *Proc. Roy. Soc. London*, *A146*, 701–722.
- Szilagyi, J., and J. Jozsa (2008), New findings about the complementary relationship-based evaporation estimation methods, *J. Hydrol.*, *354*, 171–186.
- Szilagyi, J., and J. Jozsa (2009a), Analytical solutions of the coupled 2-D turbulent heat and vapor transport equations and the complementary relationship of evaporation, *J. Hydrol.*, *372*, 61–67.
- Szilagyi, J., and J. Jozsa (2009b), An evaporation estimation method based on the coupled 2-D turbulent heat and vapor transport equations, *J. Geophys. Res.*, *114*, D06101, doi:10.1029/2008JD010772.
- Szilagyi, J., M. Hobbins, and J. Jozsa (2009), A modified advection-aridity model of evapotranspiration, *J. Hydrol. Eng.*, *14*(6), 569–574.